

From One Single Sketch to 3D Detailed Face Reconstruction

LITING WEN*, Carnegie Mellon University, USA

ZIMO YANG*, Nanyang Technological University, Singapore

XIANLIN ZHANG, Beijing University of Posts and Telecommunications, China

CHI DING, Beijing University of Posts and Telecommunications, China

MINGDAO WANG, Tsinghua University, China

XUEMING LI, Beijing University of Posts and Telecommunications, China

3D face reconstruction from a single sketch is a critical yet underexplored task with significant practical applications. The primary challenges stem from the substantial modality gap between 2D sketches and 3D facial structures, including: (1) accurately extracting facial keypoints from 2D sketches; (2) preserving diverse facial expressions and fine-grained texture details; and (3) training a high-performing model with limited data. In this paper, we propose Sketch-1-to-3, a novel framework for realistic 3D face reconstruction from a single sketch, to address these challenges. Specifically, we first introduce the Geometric Contour and Texture Detail (GCTD) module, which enhances the extraction of geometric contours and texture details from facial sketches. Additionally, we design a deep learning architecture with a domain adaptation module and a tailored loss function to align sketches with the 3D facial space, enabling high-fidelity expression and texture reconstruction. To facilitate evaluation and further research, we construct SketchFaces, a real hand-drawn facial sketch dataset, and Syn-SketchFaces, a synthetic facial sketch dataset. Extensive experiments demonstrate that Sketch-1-to-3 achieves state-of-the-art performance in sketch-based 3D face reconstruction.

CCS Concepts: • **Computing methodologies** → **Reconstruction**; *Image processing*; • **Applied computing** → Fine arts.

Additional Key Words and Phrases: Sketch-based modeling, 3D face reconstruction, High-fidelity, Single sketch, Face sketch dataset

1 INTRODUCTION

3D face reconstruction from a single sketch has attracted considerable attention due to its wide-ranging applications, including animation creation [31], face recognition [29], model retrieval [32], and facial texture generation [30]. Although many existing works have focused on reconstructing 3D faces from richly informative images, the task of reconstructing high-fidelity 3D faces from a single hand-drawn sketch remains significantly more challenging. Unlike real images, sketches inherently contain sparse information, abstract representations, and user-specific stylistic variances, making accurate 3D reconstruction particularly difficult. Achieving a satisfying reconstruction from a single sketch involves faithfully capturing intended geometric contours and subtle facial details without introducing misleading embellishments or omissions.

Specifically, despite significant advancements in separate sketch-to-image and image-to-3D face reconstruction methods, we observe that naively combining these two methods for sketch-to-3D face reconstruction introduces a significant amount of misleading information that is not inherently associated with the original sketch, thus impeding a faithful reconstruction of the user’s original intent, as illustrated in Figure 2. This observation highlights a critical limitation of existing pipelines: they are not designed to handle the unique challenges of directly reconstructing 3D faces from sketches, where the input is sparse, abstract, and rich in user-specific stylistic variances. Therefore, a

*Both authors contributed equally to this research.

Authors’ addresses: Liting Wen, Carnegie Mellon University, Pittsburgh, USA; Zimo Yang, Nanyang Technological University, Singapore, Singapore; Xianlin Zhang, Beijing University of Posts and Telecommunications, Beijing, China; Chi Ding, Beijing University of Posts and Telecommunications, Beijing, China; Mingdao Wang, Tsinghua University, Beijing, China; Xueming Li, Beijing University of Posts and Telecommunications, Beijing, China.

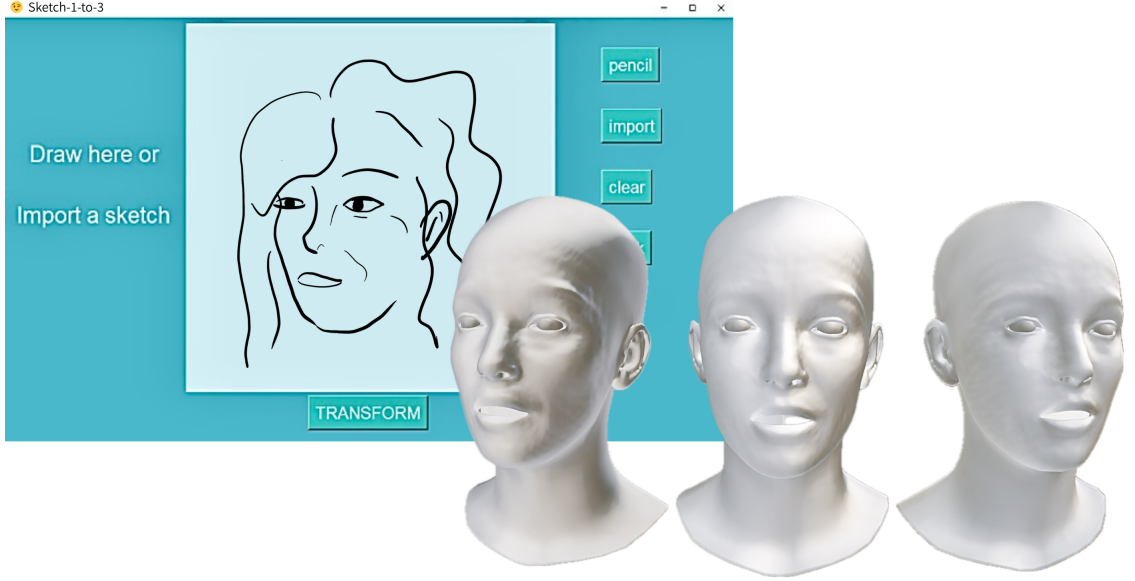


Fig. 1. A user creates a single facial sketch using our Sketch-1-to-3 system (left). The system produces a detailed 3D face reconstruction (right) that faithfully captures the sketch’s intended geometry and fine details, and is robust to occlusions, clutter, and diverse stylistic stroke variations.

dedicated sketch-to-3D face reconstruction framework is desirable and essential. In this paper, we present a novel method specifically tailored to minimize misleading artifacts while preserving essential geometric structures and facial details, enabling faithful recovery of the user’s original intent.

We identify key limitations in sketch-based 3D face reconstruction, including the inherent ambiguity of hand-drawn sketches that hinders reliable information extraction, the difficulty of reconstructing high-fidelity 3D faces with vivid expressions and fine details from abstract line drawings, and the scarcity of high-quality facial sketch datasets for training. To overcome these challenges, we introduce Sketch-1-to-3, a novel framework that reconstructs high-fidelity 3D faces from a single sketch by accurately extracting contours and facial details. Furthermore, to address the data scarcity problem, we contribute two datasets: SketchFaces, a real hand-drawn sketch dataset encompassing diverse drawing styles, and Syn-SketchFaces, a synthetic dataset generated through a carefully designed synthesis pipeline.

In summary, our main contributions are:

- We propose an end-to-end framework, Sketch-1-to-3, for high-fidelity 3D face reconstruction from a single sketch. Our method is the first to explicitly address the precise transmission of information within a single sketch, enabling the reconstruction of a 3D face model with both accurate contours and fine-grained details.
- We introduce a novel enhancement **G**eometric **C**ontour and **T**exture **D**etail (GCTD) module, which effectively extracts accurate geometric structures and fine details from sketches. We further design a domain adaption module and a task-specific loss function to seamlessly align 2D sketches with 3D space, ensuring expressive and detail-preserving 3D face reconstruction.

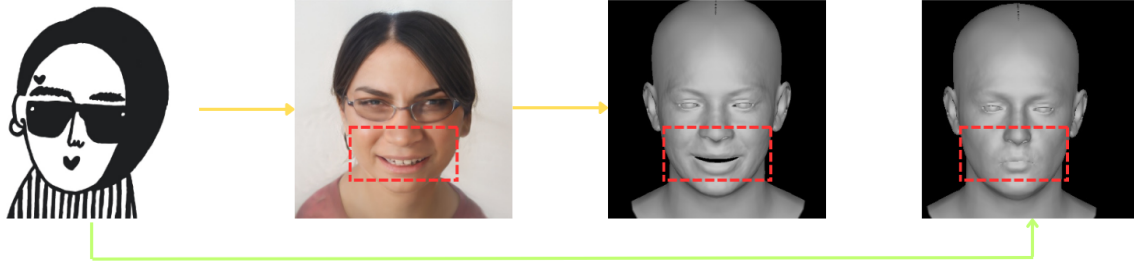


Fig. 2. Challenge demonstration. We employ[19] to transform the input sketch into the photo and then use[6] to generate the 3D face from the obtained photo, as elucidated by the yellow line. The green line signifies our method. It is apparent that employing the circuitous sketch-photo-3D (yellow line) method may give rise to reconstruction bias.

- To address the critical data scarcity challenge in this domain, we introduce two comprehensive datasets: SketchFaces, containing real hand-drawn facial sketches, and Syn-SketchFaces, a large-scale synthetic sketch face dataset. These datasets can significantly advance research in sketch-based 3D face learning.
- Extensive experiments show that Sketch-1-to-3 achieves state-of-the-art result in sketch-based 3D face reconstruction compared with previous methods.

2 RELATED WORK

2.1 Monocular 3D Face Reconstruction

Reconstructing 3D faces from a single 2D image is an inherently ill-posed problem, requiring supplementary prior knowledge to constrain the reconstruction process. A widely adopted approach is to estimate the parameters of a 3D Morphable Model [2]. Existing methods can be broadly categorized into optimization-based [1, 10, 22, 28, 36] and learning-based techniques [5, 6, 12, 23, 24]. A major challenge for learning-based methods is the lack of ground-truth 2D–3D paired data. Inspired by [25], which shows that accurate 3D face reconstruction is possible without 3D supervision using synthetic data, we propose a sketch-based method that reconstructs detailed 3D faces from a single sketch using only 2D supervision on real and synthetic data.

2.2 Sketch-based 2D Face Generation

There has been significant progress in converting free-hand sketches into realistic 2D face images. To bridge cross-modal gaps in sketch-to-photo synthesis, GLAS [17] adopts a global-local fusion network within a few-shot asymmetric translation framework. SC-FEGAN [11] generates images when users provide free-form masks, sketches, and colors as input. DrawingInStyles [26] incorporates spatial constraints from sketches and semantic maps into StyleGAN [13] to achieve high-quality and editable 2D face generation. DeepFacePencil [16] employs spatial attention pooling and a dual-generator design to adaptively reconcile the domain differences between sketches and face images, allowing generalization to freehand inputs. While these methods effectively translate facial sketches into 2D images using multimodal strategies, they remain limited to 2D generation without addressing detailed 3D face reconstruction. Building on these insights, we take a step further by reconstructing a 3D face from a single sketch.

2.3 Sketch-based 3D Face Reconstruction

Although 2D sketch-to-face generation has advanced considerably, reconstructing 3D faces directly from sketches remains underexplored. DeepSketch2Face [8] introduces a deep learning-based system that reconstructs 3D caricature-style faces from sketches. While it enables rapid generation of facial geometry and expressions from free-hand inputs, the results are often cartoonish and lack fine-grained details, limiting its applicability to high-fidelity 3D face reconstruction. SketchFaceNeRF [19] requires significant training time and fails to recover complete geometry from a single sketch, yielding only partial-view models. A subsequent work [33] proposes a two-stage method that first combines sketches and reference photos for coarse reconstruction, then refines the 3D face with sketch contours. However, the results still fail to produce detailed 3D faces. Motivated by these limitations, we propose Sketch-1-to-3, a novel framework for reconstructing the high-fidelity 3D face from a single sketch by explicitly capturing and transmitting structural cues to recover both accurate contours and fine-grained details.

3 METHOD

Our goal is to reconstruct the 3D detailed face from a single sketch. Face sketches often exhibit two traits: (1) unrestrained composition that may deviate from real-face symmetry, necessitating adaptability to varying styles and distortions; and (2) strokes that mix noise with critical intentions from the creator, highlighting the need for noise suppression and critical feature enhancement. Motivated by these observations, we propose a sketch-to-3D detailed face reconstruction method with a novel feature enhancement module, as shown in Figure 3, aiming to facilitate the recognition of sketches while accentuating finer details embedded in sketches. Notably, our method exclusively relies on 2D training data, thus circumventing the limitations associated with the lack of 3D training data. Detailed settings are provided in the *Supplementary Material*.

3.1 Preliminaries

Since reconstructing 3D face from single sketch is ill-posed, we combine the prior knowledge from FLAME[15], a 3D head model that separates the representation of identity shape β , pose parameters θ , and expression components ψ . It can be defined as

$$M(\beta, \theta, \psi) : \mathbb{R}^{|\beta| \times |\theta| \times |\psi|} \rightarrow \mathbb{R}^{3N}, \quad (1)$$

where N denotes 5023 vertices. We estimate the FLAME parameters $\beta \in \mathbb{R}^{100}$, $\theta \in \mathbb{R}^6$, $\psi \in \mathbb{R}^{50}$, albedo parameters $\alpha \in \mathbb{R}^{50}$, Spherical Harmonics (SH) lighting $l \in \mathbb{R}^{27}$, and camera model $c \in \mathbb{R}^3$ for each input sketch.

Note that α helps gain FLAME’s texture map $A(\alpha) \in \mathbb{R}^{d \times d \times 3}$ using an appearance model, which is converted from Basel Face Model’s linear albedo space to the FLAME UV layout. Camera information c helps project 3D vertices to the 2D space, consisting of isotropic scale $s \in \mathbb{R}$ and 2D translation $t \in \mathbb{R}^2$. Using the differentiable renderer R [7], we can obtain the rendering result as

$$R(M, \alpha, l, c) \rightarrow I_g, \quad (2)$$

where I_g denotes the 2D sketch generated from the 3D shape.

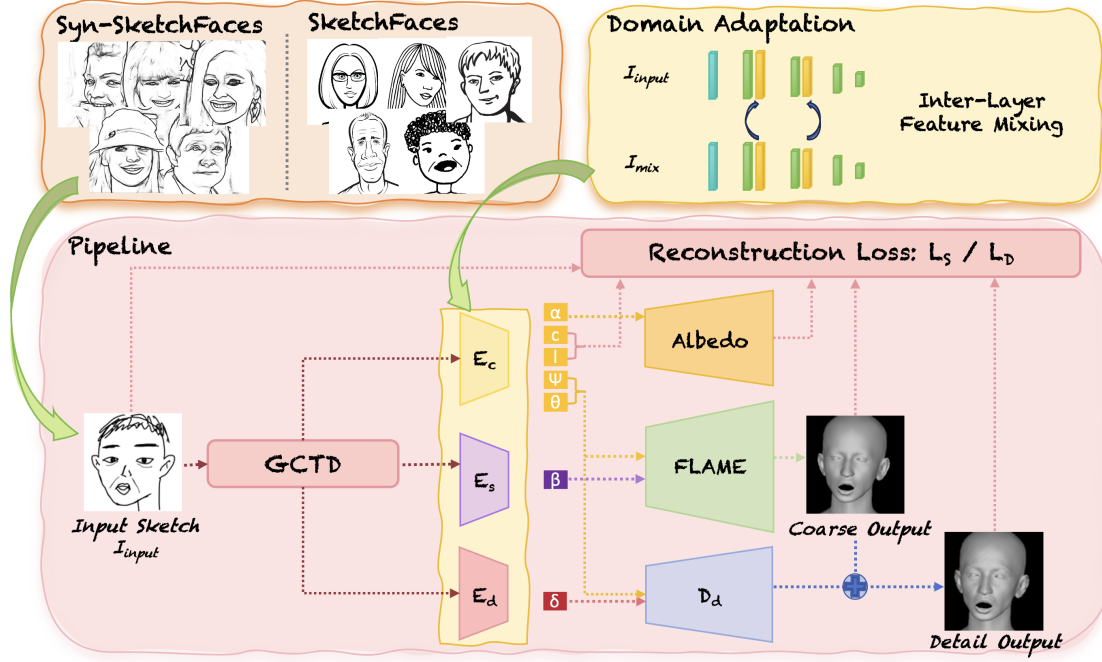


Fig. 3. An overview of the proposed method, which consists of coarse and detail training stages. In the coarse stage, a shape encoder E_s regresses β and a coarse encoder E_c regresses θ , ψ , l , c , and α . In the detail stage, a detail encoder E_d generates a latent code δ to refine the coarse 3D face with fine details. The 3D faces from both stages are rendered into 2D and compared with the input sketch to compute reconstruction losses. A GCTD module is applied in both stages to enhance feature extraction. All encoders employ inter-layer feature mixing for domain adaptation.

3.2 Enhancement Module of GCTD

The feature enhancement module of GCTD (Geometric Contour and Texture Detail) strengthens sketch features by improving contour detection and refining facial details, ensuring higher-quality representations for subsequent encoders. This non-learning module effectively resolves ambiguity in sketch facial features.

The input sketch is first denoised using bilateral filtering, a non-linear, edge-preserving smoothing method that jointly considers spatial proximity h_s and intensity similarity h_r . The process is defined as:

$$g(x, y) = \frac{1}{W} \sum_{a, b} f(x + a, y + b) \cdot h_s \cdot h_r \quad (3)$$

where W is the normalization factor, $f(x, y)$ represents the processed pixels in the image, (a, b) represents the size of the filter. This suppresses noise while preserving prominent facial contours. To further reduce detail loss, the range parameter that governs h_r is adaptively adjusted according to local variance, sharpening edges in high-frequency regions while enhancing smoothing in homogeneous areas. The resulting sketch is cleaner and structurally consistent, enabling more robust feature extraction in subsequent stages.

Subsequently, the sketch is enhanced by balancing the image to make it clearer. The process is defined as

$$s = T(r) = \int_0^r p(r) dr, \quad (4)$$

where r represents the original image grayscale, s represents the transformed image grayscale, and $p(r)$ is the probability of the occurrence of r . The sketches have more distinct features after being processed by the GCTD module, which is designed with the explicit intention of not producing a realistic image as an intermediate state. The sketches with enhanced features are used for the later facial contour detection, providing a relatively more economical alternative in terms of computational cost.

3.3 Loss Function

Weighted Landmark Loss: This Landmark loss calculates the correspondence of landmarks by compelling the projection of the 3D landmarks to align with the ground-truth landmarks of the sketch.

$$L_{lmk} = \sum_{i=1}^{68} \omega_i \|k_i - s\Pi(M_i) + t\|_1, \quad (5)$$

where $\Pi \in \mathbb{R}^{2 \times 3}$ refers to the projection matrix in the process of projecting 3D mesh into the 2D space, and $M_i \in \mathbb{R}^3$ is the corresponding vertex of FLAME model M . Different weights ω_i are assigned to landmarks in the facial regions, with the highest for the jawline and inner mouth, followed by the corners of the nose and mouth, and the lowest for other areas.

Mutual Distance Loss: Compared to L_{lmk} , the mutual distance loss is less susceptible to misalignment during the reconstruction process and can especially facilitate a more effective capture of expressions and shapes. Simply put, the mutual distance between keypoint pair P can be defined as

$$L_p = \sum_{(i,j) \in P} \|k_i - k_j - s\Pi(M_i - M_j)\|_1, \quad (6)$$

where P is a set of keypoint pairs, $k_i \in \mathbb{R}^2$ and $k_j \in \mathbb{R}^2$ refer to corresponding ground-truth 2D landmarks. Based on this definition, we opt for three categories of keypoint pairs to calculate our mutual distance loss, including keypoint pairs of eyes, inner mouth, and facial contours. To sum up, the loss computes as

$$L_{md} = \omega_{eyeP} L_{eyeP} + \omega_{mouP} L_{mouP} + \omega_{conP} L_{conP}, \quad (7)$$

where ω_x denotes the respective weight.

Photometric Loss: We use a photometric loss measuring differences between the input sketch I_{input} and the generated image I_g .

$$L_{pho} = \|V \odot (I_{input} - I_g)\|_{1,1}, \quad (8)$$

where V_1 is a face mask, and the operator \odot refers to the Hadamard product. Note that this kind of loss is calculated in both the coarse and detail stages to ensure photometric consistency. We designate them as L_{phoS} and L_{phoD} , respectively, to make a distinction.

Regularization: For the coefficients of the coarse and the detail stages, we employ their L2 regularization terms as regularization losses, denoted as L_{regS} and L_{regD} , respectively.

Overall Loss Functions: Overall, in coarse training stage, our optimization goal is

$$L_S = L_{lmk} + L_{md} + \omega_{pho} L_{phoS} + \omega_{reg} L_{regS}. \quad (9)$$

Table 1. Quantitative Comparisons. We employ two metrics, SSIM and GMSD, to evaluate the reconstruction performance of several models. The notation (\downarrow) signifies a preference for lower values, while (\uparrow) signifies a preference for higher values.

Method	SketchMetaFace[20]	SketchFaceNeRF[19]	[19]-DECA[6]	Ours
SSIM (\uparrow)	0.5399	0.5209	0.9616	0.9689
GMSD (\downarrow)	0.5569	0.5345	0.4584	0.4072

Table 2. Ablation studies on GCTD and loss functions.

Model	SSIM (\uparrow)	GMSD (\downarrow)
Sketch-1-to-3 w/o GCTD	0.9611	0.4469
Sketch-1-to-3 w/o L_{comp}	0.9676	0.4304
Sketch-1-to-3 w/o L_{md}	0.9682	0.4265
Sketch-1-to-3 w/o L_{lmk}	0.9685	0.4259
Sketch-1-to-3	0.9689	0.4072

In detail training stage, our optimization goal is

$$L_D = L_{md} + \omega_{pho} L_{phoD} + \omega_{reg} L_{regD}. \quad (10)$$

The weights of L_{pho} and L_{reg} are denoted as ω_{pho} and ω_{reg} , respectively.

3.4 Domain Adaptation

Despite incorporating real hand-drawn sketches—such as those from the CUFSF dataset [34] and our SketchFaces dataset—to enrich the training data, the scarcity of large-scale, high-quality facial sketch datasets still necessitates the use of synthetic data. To address this, we introduce Syn-SketchFaces, a synthetic dataset aimed at increasing both the diversity and volume of training samples.

However, the domain gap between synthetic and real sketches, which stems from differences in texture, stroke patterns, and abstraction levels, poses a significant challenge to the model’s generalization to real-world sketches. In addition, sketches from different sources or artists often exhibit substantial style variations, which further hinder generalization. Inspired by [4, 35], we incorporate a domain adaptation strategy into our approach, mixing feature statistics from the Syn-SketchFaces dataset and the SketchFaces dataset based on the inherent connection between image style and feature statistics[9]. During training, all encoders employ inter-layer feature mixing. We apply the mixing in lower layers, where features are most sensitive to texture, color, and stroke patterns. Let $F_l(\cdot)$ denote the encoder truncated at layer l . Given an input sketch I_{input} and another sketch for mixing I_{mix} , we obtain the feature maps $x = F_l(I_{input})$ and $x' = F_l(I_{mix})$. We then mix their channel-wise statistics at layer l as

$$\hat{x} = \left(\frac{x - \mu}{\sigma} \right) \odot (\lambda \sigma + (1 - \lambda) \sigma') + (\lambda \mu + (1 - \lambda) \mu'), \quad (11)$$

where μ, σ (resp. μ', σ') are the per-channel mean and standard deviation of x (resp. x') computed over spatial dimensions, \odot denotes channel-wise broadcasting multiplication, and λ is a per-sample mixing coefficient drawn from a symmetric Beta distribution, controlling the mixing strength.

This strategy not only bridges the gap between synthetic and real sketches but also enhances robustness to intra-domain sketch style variations, resulting in a marked performance gain on diverse sketch inputs.



Fig. 4. (a) Syn-SketchFaces generation process: from original photos to PiDiNet contours to synthetic sketches. (b) Real sketch samples from the SketchFaces dataset.

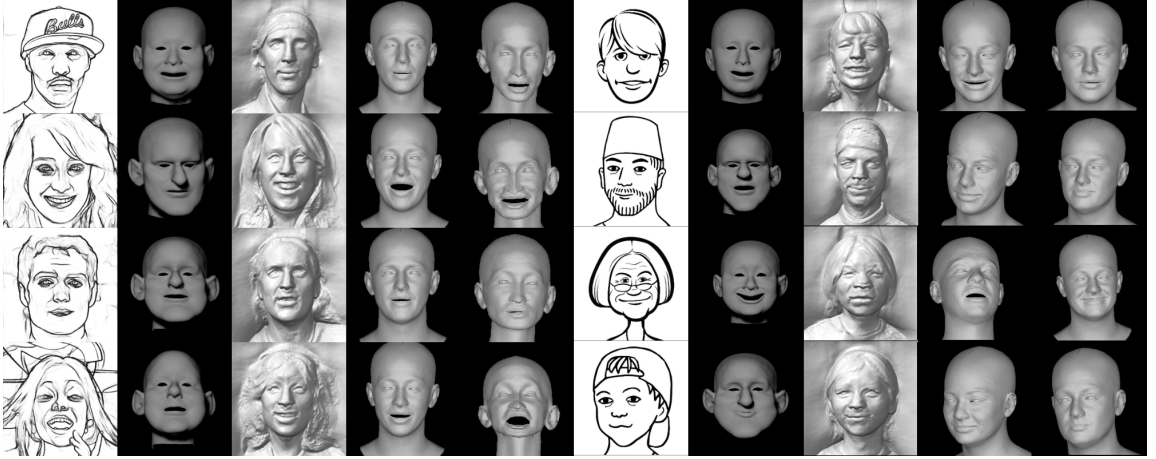


Fig. 5. Qualitative comparisons. The left half shows reconstructions from synthetic sketches, and the right half from real hand-drawn sketches. Each group of five columns includes (from left to right): (1) input sketch, (2) DeepSketch2Face[8], (3) SketchFaceNeRF[19], (4) the combination of [19] and [6], and (5) our Sketch-1-to-3.

4 EXPERIMENT

4.1 Dataset

There are currently very few facial sketch datasets available, and existing relevant datasets, such as [34], can not suffice for training robust sketch-to-3D face reconstruction models because of their limited scales. To optimize the performance of our model, we have collected a real hand-drawn sketch dataset, identified as SketchFaces. Moreover, considering there is a significant cost associated with gathering real hand-drawn sketches, we also generate the synthetic sketch dataset from facial photos. Given the relative abundance of facial photo datasets, we thus obtained a synthetic dataset

Table 3. User studies. Average ratings (scale: 1–5, poor to excellent) across four dimensions for expert (Group A) and non-expert (Group B) users.

Group	Modeling Support	Convenience	Accuracy	General Satisfaction
A	4.000	4.267	3.467	3.933
B	4.333	4.400	4.067	4.533

named Syn-SketchFaces that played a crucial role in the training phase. Furthermore, we use the methods proposed by [3, 37] to obtain facial landmarks and [21] for face segmentation, thereby labeling our datasets.

Syn-SketchFaces: We use PiDiNet [27] to extract gradient cues from images in SCUT-FBP5500 [18] and CelebAMask-HQ [14], producing sketch-like results, as shown in Figure 4a. Each original image is first processed with edge detection, followed by color inversion to generate the final sketches. The resulting dataset preserves both the facial contours and key details.

SketchFaces: We gather real hand-drawn facial sketches from individuals with varying levels of artistic proficiency and from a wide range of online sources, capturing diverse sketch styles and drawing mediums, as shown in Figure 4b.

4.2 Quantitative Comparisons

In Table 1, we quantify reconstruction results using SSIM, which measures structural similarity, and GMSD, which integrates gradient information to capture edge variations. These metrics jointly provide a comprehensive evaluation. As paired sketch–3D data are unavailable, we project the reconstructed 3D faces into 2D and compare them with the input sketches. All evaluations use the SketchFaces dataset.

4.3 Qualitative Comparisons

We conduct qualitative comparisons between our proposed method Sketch-1-to-3 and the current state-of-the-art 3D face reconstruction methods. The results demonstrate the superior performance of our method on both synthetic sketches and real hand-drawn sketches. See Figure 5. The five columns on the left illustrate the results of the 3D facial reconstruction in synthetic sketches, while the five columns on the right illustrate the results of the 3D facial reconstruction results on real hand-drawn sketches.

The results of DeepSketch2Face [8] are often abstract and cartoon-like, with limited fidelity to the details of the sketch. In contrast, our Sketch-1-to-3 more accurately captures facial structure, better aligning contours and feature positions. Although SketchFaceNeRF [19] appears detailed, many of its reconstructed details do not genuinely originate from the input sketch. Compared to this, our method avoids hallucinated content and faithfully adheres to the sketch input. Furthermore, our method shows greater robustness to occlusions such as hats, while SketchFaceNeRF struggles in such cases.

We also compare our method with a two-step alternative that combines [19] and [6], which first synthesizes 2D images from sketches and then reconstructs 3D faces. Although each method excels within its domain, the cross-modal translation, from sketch to photo to 3D, introduces inconsistencies that degrade reconstruction quality. This indirect pipeline tends to hallucinate details absent from the original sketch, making it difficult for the 3D model to capture meaningful feature, as illustrated in Figure 2. In contrast, our method produces faithful and coherent 3D reconstructions

that consistently align well with the input sketches, showing robust performance across diverse sketches. More results across diverse sketch styles are provided in the *Supplementary Material*.

4.4 Ablation Studies

Figure 6a and Figure 6b demonstrate the effectiveness of our proposed loss functions and the GCTD module. Quantitative results in Table 2 further validate their contributions.

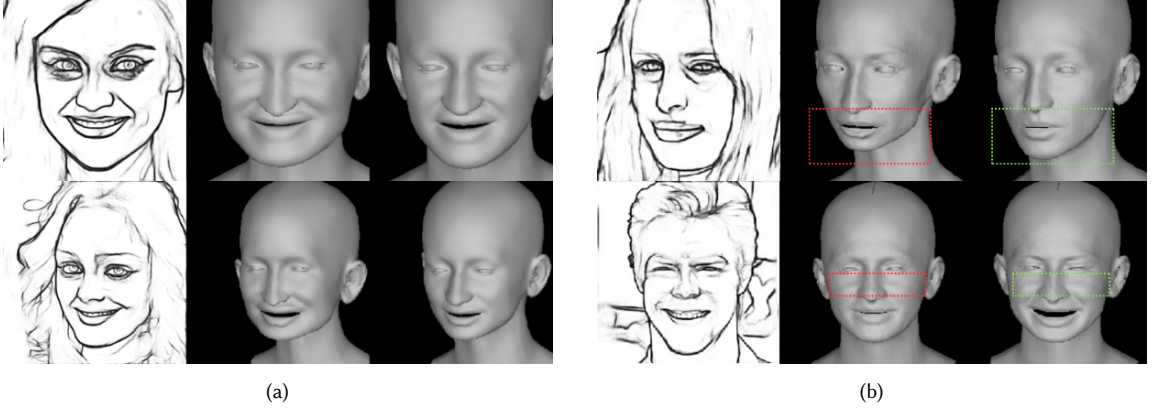


Fig. 6. Ablation studies. In (a), the first row shows the input sketch, Sketch-1-to-3 without L_{md} , and the full model; the second row shows the input sketch, Sketch-1-to-3 without L_{conP} , and the full model. In (b), both rows show the input sketch, Sketch-1-to-3 without GCTD, and the full model.

Ablation Studies on Loss Functions: We conduct ablation studies by selectively removing the loss term during training. As illustrated in the first row, second column of Figure 6a, excluding the mutual distance loss L_{md} leads to poor alignment with the input sketch, particularly in the chin area. Additionally, in the second row, we investigate L_{conP} . Its removal causes deformation in the jawline, highlighting its role in preserving facial structure.

Ablation Studies on GCTD: We conduct ablation studies by removing the GCTD module during training. In Figure 6b, the second column shows reconstructions without GCTD, while the third column includes it. The first row demonstrates improved contour alignment and the second row reveals a more faithful detail reconstruction. Moreover, GCTD helps correct misalignments caused by recognition errors. These findings highlight the performance of the module in improving reconstruction accuracy.

4.5 User Studies

We conducted a user study to evaluate the real-world applicability of our method, comparing expert users with prior 3D modeling experience to non-expert users. Detailed design and procedures for the user study are provided in the *Supplementary Material*.

The evaluation was conducted along four dimensions: (1) Modeling Support, which assesses the level of assistance provided by the system during the 3D modeling process; (2) Convenience, reflecting the ease and intuitiveness of obtaining results; (3) Accuracy, measuring the perceived correctness and realism of the reconstructed model; (4) General Satisfaction, measuring the overall user experience. As shown in Table 3, our method received favorable scores from

both expert (Group A) and non-expert (Group B) users. Notably, Group B consistently rated the system higher across all evaluation dimensions, with the most significant improvements observed in Accuracy and General Satisfaction. These results suggest that our method is particularly effective in supporting novice users, enabling them to achieve satisfactory 3D face modeling outcomes.

5 CONCLUSION

In this paper, we present Sketch-1-to-3, an end-to-end framework for high-fidelity 3D face reconstruction from a single sketch. Our method addresses the unique challenges posed by sketch-based 3D face reconstruction, including sparse and abstract representations, diverse artistic styles, and the scarcity of sketch data. By introducing the GCTD module, we effectively enhanced the extraction of facial geometry and subtle features from sketches, while our domain adaptation strategy and diverse loss function ensured precise alignment between 2D sketches and 3D reconstruction.

To further advance research in this domain, we constructed two datasets: SketchFaces and Syn-SketchFaces. Extensive experiments demonstrated that Sketch-1-to-3 achieves state-of-the-art performance, accurately capturing both coarse geometric structure and delicate details, while exhibiting robustness to occlusions, stylistic variations, and incomplete strokes. Further discussion of future work can be found in the *Supplementary Material*.

REFERENCES

- [1] Oswald Aldrian and William AP Smith. 2012. Inverse rendering of faces with a 3D morphable model. *IEEE transactions on pattern analysis and machine intelligence* 35, 5 (2012), 1080–1093.
- [2] Volker Blanz and Thomas Vetter. 2003. Face recognition based on fitting a 3D morphable model. *IEEE Transactions on pattern analysis and machine intelligence* 25, 9 (2003), 1063–1074.
- [3] Adrian Bulat and Georgios Tzimiropoulos. 2017. How far are we from solving the 2d & 3d face alignment problem?(and a dataset of 230,000 3d facial landmarks). In *Proceedings of the IEEE international conference on computer vision*. 1021–1030.
- [4] Xiaoxu Cai, Jianwen Lou, Jiajun Bu, Junyu Dong, Haishuai Wang, and Hui Yu. 2024. Single depth image 3d face reconstruction via domain adaptive learning. *Frontiers of Computer Science* 18, 1 (2024), 181342.
- [5] Yu Deng, Jiaolong Yang, Sicheng Xu, Dong Chen, Yunde Jia, and Xin Tong. 2019. Accurate 3d face reconstruction with weakly-supervised learning: From single image to image set. In *Proceedings of the IEEE/CVF conference on computer vision and pattern recognition workshops*. 0–0.
- [6] Yao Feng, Haiwen Feng, Michael J Black, and Timo Bolkart. 2021. Learning an animatable detailed 3D face model from in-the-wild images. *ACM Transactions on Graphics (ToG)* 40, 4 (2021), 1–13.
- [7] Kyle Genova, Forrester Cole, Aaron Maschinot, Aaron Sarna, Daniel Vlasic, and William T Freeman. 2018. Unsupervised training for 3d morphable model regression. In *Proceedings of the IEEE Conference on Computer Vision and Pattern Recognition*. 8377–8386.
- [8] Xiaoguang Han, Chang Gao, and Yizhou Yu. 2017. DeepSketch2Face: a deep learning based sketching system for 3D face and caricature modeling. *ACM Transactions on graphics (TOG)* 36, 4 (2017), 1–12.
- [9] Xun Huang and Serge Belongie. 2017. Arbitrary style transfer in real-time with adaptive instance normalization. In *Proceedings of the IEEE international conference on computer vision*. 1501–1510.
- [10] Patrik Huber, Zhen-Hua Feng, William Christmas, Josef Kittler, and Matthias Rätzsch. 2015. Fitting 3d morphable face models using local features. In *2015 IEEE international conference on image processing (ICIP)*. IEEE, 1195–1199.
- [11] Youngjoo Jo and Jongyoul Park. 2019. Sc-fegan: Face editing generative adversarial network with user’s sketch and color. In *ICCV*. 1745–1753.
- [12] Amin Jourabloo and Xiaoming Liu. 2016. Large-pose face alignment via CNN-based dense 3D model fitting. In *Proceedings of the IEEE conference on computer vision and pattern recognition*. 4188–4196.
- [13] Tero Karras, Samuli Laine, and Timo Aila. 2019. A style-based generator architecture for generative adversarial networks. In *Proceedings of the IEEE/CVF conference on computer vision and pattern recognition*. 4401–4410.
- [14] Cheng-Han Lee, Ziwei Liu, Lingyun Wu, and Ping Luo. 2020. Maskgan: Towards diverse and interactive facial image manipulation. In *Proceedings of the IEEE/CVF conference on computer vision and pattern recognition*. 5549–5558.
- [15] Tianye Li, Timo Bolkart, Michael J Black, Hao Li, and Javier Romero. 2017. Learning a model of facial shape and expression from 4D scans. *ACM Trans. Graph.* 36, 6 (2017), 194–1.
- [16] Yuhang Li, Xuejin Chen, Binxin Yang, Zihan Chen, Zhihua Cheng, and Zheng-Jun Zha. 2020. Deepfacepencil: Creating face images from freehand sketches. In *Proceedings of the 28th ACM International Conference on Multimedia*. 991–999.
- [17] Yongkang Li, Qifan Liang, Zhen Han, Wenjun Mai, and Zhongyuan Wang. 2024. Few-shot face sketch-to-photo synthesis via global-local asymmetric image-to-image translation. *ACM Transactions on Multimedia Computing, Communications and Applications* 20, 10 (2024), 1–24.
- [18] Lingyu Liang, LuoJun Lin, Lianwen Jin, Duorui Xie, and Mengru Li. 2018. SCUT-FBP5500: A diverse benchmark dataset for multi-paradigm facial beauty prediction. In *2018 24th International conference on pattern recognition (ICPR)*. IEEE, 1598–1603.
- [19] Gao Lin, Liu Feng-Lin, Chen Shu-Yu, Jiang Kaiwen, Li Chunpeng, Yukun Lai, and Fu Hongbo. 2023. SketchFaceNeRF: Sketch-based facial generation and editing in neural radiance fields. *ACM Transactions on Graphics* (2023).
- [20] Zhongjin Luo, Dong Du, Heming Zhu, Yizhou Yu, Hongbo Fu, and Xiaoguang Han. 2023. SketchMetaFace: A Learning-based Sketching Interface for High-fidelity 3D Character Face Modeling. *IEEE Transactions on Visualization and Computer Graphics* (2023).
- [21] Yuval Nirkin, Iacopo Masi, Anh Tran Tuan, Tal Hassner, and Gerard Medioni. 2018. On face segmentation, face swapping, and face perception. In *2018 13th IEEE International Conference on Automatic Face & Gesture Recognition (FG 2018)*. IEEE, 98–105.
- [22] Stylianos Ploumpis, Evangelos Ververas, Eimear O’Sullivan, Stylianos Moschoglou, Haoyang Wang, Nick Pears, William AP Smith, Baris Gecer, and Stefanos Zafeiriou. 2020. Towards a complete 3D morphable model of the human head. *IEEE transactions on pattern analysis and machine intelligence* 43, 11 (2020), 4142–4160.
- [23] Elad Richardson, Matan Sela, Roy Or-El, and Ron Kimmel. 2017. Learning detailed face reconstruction from a single image. In *Proceedings of the IEEE conference on computer vision and pattern recognition*. 1259–1268.
- [24] Soubhik Sanyal, Timo Bolkart, Haiwen Feng, and Michael J Black. 2019. Learning to regress 3D face shape and expression from an image without 3D supervision. In *Proceedings of the IEEE/CVF Conference on Computer Vision and Pattern Recognition*. 7763–7772.
- [25] Matan Sela, Elad Richardson, and Ron Kimmel. 2017. Unrestricted facial geometry reconstruction using image-to-image translation. In *Proceedings of the IEEE international conference on computer vision*. 1576–1585.
- [26] Wanchao Su, Hui Ye, Shu-Yu Chen, Lin Gao, and Hongbo Fu. 2022. Drawinginstyles: Portrait image generation and editing with spatially conditioned stylegan. *IEEE TVCG* (2022).
- [27] Zhuo Su, Wenzhe Liu, Zitong Yu, Dewen Hu, Qing Liao, Qi Tian, Matti Pietikäinen, and Li Liu. 2021. Pixel difference networks for efficient edge detection. In *Proceedings of the IEEE/CVF international conference on computer vision*. 5117–5127.

- [28] Justus Thies, Michael Zollhofer, Marc Stamminger, Christian Theobalt, and Matthias Nießner. 2016. Face2face: Real-time face capture and reenactment of rgb videos. In *Proceedings of the IEEE conference on computer vision and pattern recognition*. 2387–2395.
- [29] Mei Wang, Ruizhuo Xu, Weihong Deng, and Hua Huang. 2025. Implicit face model: Depth super-resolution for 3D face recognition. *Pattern Recognition* 162 (2025), 111353.
- [30] Zidu Wang, Xiangyu Zhu, Jiang Yu, Tianshuo Zhang, and Zhen Lei. 2024. S2td-face: Reconstruct a detailed 3d face with controllable texture from a single sketch. In *Proceedings of the 32nd ACM International Conference on Multimedia*. 6453–6462.
- [31] Rongliang Wu, Yingchen Yu, Fangneng Zhan, Jiahui Zhang, Xiaoqin Zhang, and Shijian Lu. 2023. Audio-driven talking face generation with diverse yet realistic facial animations. *Pattern Recognition* 144 (2023), 109865.
- [32] Hairui Yang, Ning Wang, Zhihui Wang, and Lei Wang. 2024. Sketch-based 3D Model Retrieval with Cross-Modal Representation. In *Proceedings of the 6th ACM International Conference on Multimedia in Asia*. 1–5.
- [33] Li Yang, Jing Wu, Jing Huo, Yu-Kun Lai, and Yang Gao. 2021. Learning 3D face reconstruction from a single sketch. *Graphical Models* 115 (2021), 101102.
- [34] Wei Zhang, Xiaogang Wang, and Xiaoou Tang. 2011. Coupled information-theoretic encoding for face photo-sketch recognition. In *CVPR 2011*. IEEE, 513–520.
- [35] Kaiyang Zhou, Yongxin Yang, Yu Qiao, and Tao Xiang. 2023. Mixstyle neural networks for domain generalization and adaptation. *International Journal of Computer Vision* (2023), 1–15.
- [36] Xiangyu Zhu, Zhen Lei, Junjie Yan, Dong Yi, and Stan Z Li. 2015. High-fidelity pose and expression normalization for face recognition in the wild. In *Proceedings of the IEEE conference on computer vision and pattern recognition*. 787–796.
- [37] Zhiming Zou, Dian Jia, and Wei Tang. 2025. Towards unsupervised learning of joint facial landmark detection and head pose estimation. *Pattern Recognition* (2025), 111393.